Tectonophysics 629 (2014) 211–223

Contents lists available at ScienceDirect

Tectonophysics

journal homepage: www.elsevier.com/locate/tecto

Deformation microstructures and magnetite texture development in synthetic shear zones

Jessica L. Till *, Bruce M. Moskowitz

Institute for Rock Magnetism, University of Minnesota, 100 Union St SE, Minneapolis, MN 55455, USA

ARTICLE INFO

Article history:
Received 3 October 2013
Received in revised form 5 March 2014
Accepted 17 April 2014
Available online 26 April 2014

Keywords:
Experimental deformation
Magnetite
Magnetic anisotropy
Texture
Deformation mechanisms

ABSTRACT

We present observations of deformation features in magnetite from synthetic magnetite-bearing silicate aggregates deformed between 1000 °C and 1200 °C in transpressional shear experiments with strains of up to 300%. Anisotropy of magnetic susceptibility and shape preferred orientation (SPO) analysis were combined with electron backscatter diffraction (EBSD) to characterize the magnetite deformation fabrics and intragrain microstructures. Crystallographic preferred orientation (CPO) in magnetite is very weak in all deformed samples and does not vary as a function of either temperature or shear strain. Magnetic anisotropy and SPO increase strongly with both strain and deformation temperature and indicate that strain partitioning between magnetite and the plagioclase matrix decreases at higher temperatures. EBSD orientation mapping of individual magnetite particles revealed substantial dispersions in intragrain orientation, analogous to undulose extinction, after deformation at 1000 and 1100 °C, indicating that dislocation creep processes were active in magnetite despite the lack of a well-developed CPO. Geometrical analysis of crystallographic orientation dispersions from grain map data indicates that low-angle grain boundary formation in magnetite could have been accommodated by slip on {110} or {100} planes, but no evidence for dominant slip on the expected {111} planes was found. Evidence for activation of multiple slip systems was seen in some magnetite grains and could be partially responsible for the lack of CPO in magnetite. These results suggest that, at least in polyphase rocks, crystallographic textures in magnetite may be inherently weak or slow to develop and CPO alone is not an adequate indicator of magnetite deformation mechanisms. These results may aid in the interpretation of deformation textures in other spinel-structured phases such as chromite and ringwoodite.

1. Introduction

Magnetite is a common accessory mineral in a wide range of crustal rocks and is an important component of some iron ore bodies (Barbosa and Lagoeiro, 2010; Morales et al., 2008). Magnetite is also uniquely important to tectonics and structural geology studies that use magnetic anisotropy techniques as a petrofabric indicator since it is strongly ferromagnetic and often dominates magnetic anisotropy signatures when present (Borradaile and Jackson, 2004). However, interpretation of magnetic anisotropy in magnetite-bearing rocks can be improved with better constraints on magnetite deformation behavior during metamorphism.

A limited number of deformation experiments have previously been performed on magnetite aggregates and single crystals (Crouch and Robertson, 1990; Gómez-García et al., 2002; Hennig-Michaeli and Siemes, 1975, 1982; Muller and Siemes, 1972) and Till and Moskowitz (2013) recently proposed a revised set of flow laws for magnetite that can help to predict magnetite deformation behavior over a range of metamorphic conditions. Plastically deformed magnetite in tectonic settings has been reported in a handful of field studies (e.g. Agar and Lloyd, 1997; Ferré et al., 2003; Housen et al., 1995; Mamtani et al., 2007) but the conditions of paleostresses and strain rates can be difficult to determine in natural rocks. Mineral microstructures and crystallographic textures are often used to infer the mechanisms of deformation in naturally deformed rocks, and the development of electron backscatter diffraction (EBSD) techniques in recent decades has enabled rapid and precise determination of mineral textures. While previous experimental deformation studies have examined crystallographic texture development in magnetite using neutron diffraction methods, no experimental studies have yet used EBSD to document texture development in magnetite or any other spinel mineral.

We present an integrated study combining anisotropy of magnetic susceptibility (AMS), shape-preferred orientation (SPO), and EBSD analysis of intragrain microstructures and crystallographic textures in plastically deformed magnetite from high-temperature laboratory shear experiments. We show that despite evidence for magnetite having deformed primarily by dislocation creep in most experiments, no clear crystallographic preferred orientation (CPO) could be detected in the texture measurements for those samples.

* Corresponding author at: Helmholtz-Zentrum GFZ Potsdam, Telegrafenberg, 14473 Potsdam, Germany.
E-mail address: till@gfz-potsdam.de (J.L. Till).

http://dx.doi.org/10.1016/j.tecto.2014.04.026
0040-1951/

The present experiments were designed to study the development of magnetic anisotropy during high-temperature deformation. Thus, the experiment design is not necessarily ideal for studying the relationship between deformation mechanisms and crystallographic textures in magnetite, since no mechanical information on magnetite strength was obtained. However, the observations made here represent a novel examination of deformation features in magnetite and raise interesting questions about the nature of crystallographic texture development in magnetite and other spinel minerals.

2. Experimental and analytical procedures

2.1. Sample synthesis

Samples for deformation were created by mixing synthetic magnetite powder (Wright Industries 041183) and powdered Beaver Bay anorthosite, consisting almost purely of plagioclase with a composition near An_{70} (Morrison et al., 1983). The plagioclase was sieved to remove the coarse-grained fraction above 64 μm and washed in concentrated acid to dissolve any residual magnetic material. The magnetite has a mean grain size of 18.3 ± 12 μm and a mean grain aspect ratio of 1.6 (Yu et al., 2002). Sample powders were composed of 3 wt.% magnetite dispersed in the plagioclase matrix material (≈1.5 vol.%). The magnetite purity and the absence of Fe-bearing phases in the plagioclase were verified before synthesis through magnetic property measurements. The rock magnetic properties of the samples analyzed in this study were described in detail by Till et al. (2012). After thorough mixing, sample powders were isostatically cold-pressed under a confining pressure of 130 MPa in an oil-medium pressure vessel to avoid imparting any strong initial fabric to the samples prior to deformation. This cold-pressing step resulted in a solid pellet that was shaped and fitted into a pre-oxidized Ni canister which served as an f_{O_2} buffer. Sample-filled Ni canisters were annealed in a hot isostatic press (HIP) in an Ar-gas-medium apparatus (Paterson, 1990) at 1200 °C with a confining pressure of 300 MPa for 3 h.

Significant chemical changes occurred in the magnetite during initial hot-pressing due to cation exchange between the plagioclase matrix and magnetite grains. Electron microprobe analysis (EMPA) of the synthesized samples indicates that the opaque grains in the hot-pressed material are Fe-oxides containing approximately 5 wt.% Al based on analyses of several grains (Till et al., 2012). Microprobe analysis also revealed that the oxide grains are surrounded by rims composed of Al–Ca–Na-silicate which are depleted in Al and Ca but enriched in Si and Na relative to the silicate matrix. These rims are not visible in reflected light microscopy, and are probably plagioclase of a more albitic composition. The average oxide composition compared with matrix and rim composition is reported in Till et al. (2012). Al^{3+} substitutes for Fe^{3+} in the magnetite–hercynite solid solution according to the formula $Al_xFe_{3-x}O_4$ where $x = 0$ for pure magnetite with the inverse spinel structure and $x = 2$ corresponds to hercynite with the normal spinel structure. The oxide phase in our hot-pressed samples has a composition around $x = 0.4$ and will be referred to as magnetite for simplicity. Some difference in mechanical behavior may be expected due to the aluminum content than that of pure magnetite. EMPA was repeated in representative oxide grains post-deformation, and showed that further compositional changes after deformation were relatively minor, although Al contents were slightly higher in magnetite grains from samples deformed at 1200 °C. Microprobe analysis did not detect any compositional zoning or gradients in Fe or Al content from compositional profiles across several magnetite grains, either before or after deformation.

2.2. Deformation procedures

After hot-pressing, all metallic material from the Ni canister was removed from the sample by cutting and grinding, and the sample material was cut into disks of 1 mm thickness. Sample disks were shaped to fit the elliptical cross-section of the pistons, which were made from 5 mm-diameter alumina rod cut at a 45° angle (Fig. 1). The alumina pistons and sample disk were enclosed in a Ni jacket that was pre-oxidized by heating in air at 1200 °C for several hours. A NiO layer on the interior surface of the jacket was visible after most deformation runs, indicating that the oxygen fugacity was maintained near the Ni–NiO buffer during deformation. The full sample assembly included larger alumina and zirconia pistons on either side of the small angled pistons, all of which was enclosed in a thin Fe jacket.

Experiments were performed in an Ar-medium deformation apparatus (Paterson, 1990) at temperatures of 1000°, 1100°, and 1200 °C. Samples were deformed to shear strains, γ, in the range $\gamma = 1$–3 under a confining pressure of 300 MPa and a constant piston displacement rate between 0.06 and 0.11 μm/s, which produces approximately constant shear strain rates around $1 \times 10^{-4}\,s^{-1}$ (Table 1). Shear strains were calculated from total piston displacements using the piston geometry and sample thickness. Although the deformation geometry includes a small component of pure shear, the thinness of the samples tends to minimize the amount of flattening strain, so sample strains were approximated as solely due to simple shear. Temperatures varied by ±5 °C of the target temperature during deformation and the applied piston load automatically varied as necessary to maintain a constant strain rate. The shear stresses, τ, during the experiments were determined by applying an internal load cell correction and a correction for

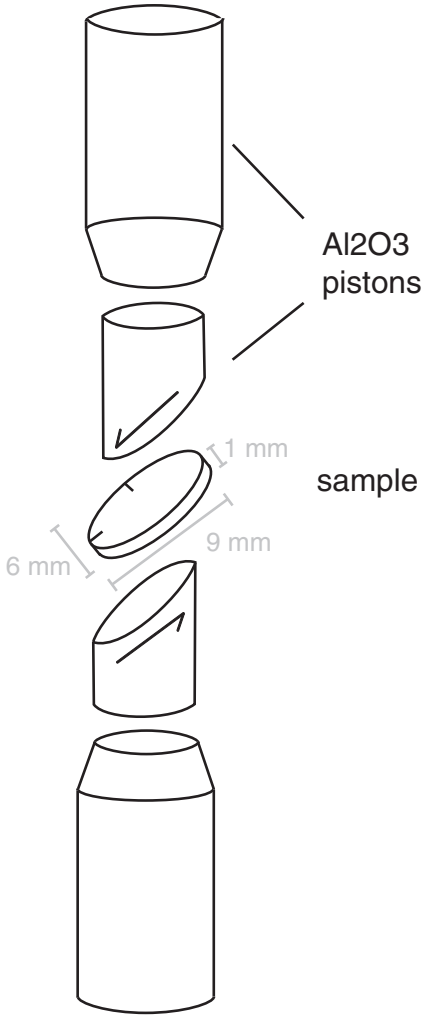

Fig. 1. Schematic diagram of sample dimensions and experimental assembly set-up for transpressional shear experiments.